applied optics

Improved measurement accuracy of spot position on an InGaAs quadrant detector

Jiabin Wu,[1,2] Yunshan Chen,[1] Shijie Gao,[1,2] Yimang Li,[1] and Zhiyong Wu[1,*]

[1]Changchun Institute of Optics, Fine Mechanics and Physics, Chinese Academy of Sciences, Changchun, Jilin 130033, China
[2]University of Chinese Academy of Science, Beijing 100049, China
*Corresponding author: wuzy@ciomp.ac.cn

Received 13 July 2015; revised 18 August 2015; accepted 19 August 2015; posted 19 August 2015 (Doc. ID 245806); published 11 September 2015

In this paper, a new formula is proposed to improve the accuracy of spot position measurements on an InGaAs quadrant detector (QD). It is obtained by analyzing the relationship between the light spot position and the output signals of the QD and combining the infinite integral method with the Boltzmann method due to their opposite error characteristics. Based on the proposed formula, the measurement accuracy can be improved greatly, which is confirmed by the simulation and experimental results. In addition, it requires fewer parameters compared with the polynomial method when reaching the same accuracy. Thus, the new formula can be practical in applications of spot position measurements.

OCIS codes: (040.5160) Photodetectors; (040.1880) Detection; (280.3420) Laser sensors; (280.4788) Optical sensing and sensors.

http://dx.doi.org/10.1364/AO.54.008049

1. INTRODUCTION

The 1550 nm wavelength laser is widely used in laser communication systems and laser radar systems because it is less affected by atmospheric turbulence than lasers of other wavelengths [1–4]. The position feedback elements in these systems are usually charge-coupled devices (CCDs), lateral effect position sensitive detectors (LEPSDs), and quadrant detectors (QDs). However, for the 1550 nm wavelength, the CCD is known to exhibit low quantum efficiency and the LEPSD has high dark current noise level, both of which are limited by the fabrication methods of these devices [5,6]. The InGaAs QD is a solution to these problems and is also advantageous in terms of its higher resolution and faster response speed, which enable high-precision position measurements and tracking [7]. Recently, QDs are also deployed in atomic force microscopy [8], high-precision photoelectric instruments, and photoelectric autocollimators [9,10].

However, according to the conventional definition of output signal offset (OSO) [11], the relationship between the spot position and the OSO is nonlinear, which means that the QD measurement has high accuracy only when the spot is near the detector center and the accuracy decreases when the spot is far from the center [12,13]. Cui *et al.* succeed in achieving higher measurement accuracy by means of modifying the definition of OSO to improve the linearity index [14], but the higher accuracy increases the complexity of the algorithm. In addition, in [8] and [15], a method by fitting the measurement data to a polynomial model has been reported to reduce the nonlinearity. Although the method can improve the measurement accuracy, a large amount of model parameters are created and it is time consuming.

This paper analyzes the relationship between the spot position and the output signals of the QD illuminated by a Gaussian profile laser beam. A new formula is proposed to estimate the spot position with reduced nonlinearity. It combines the infinite integral method with the Boltzmann method due to their opposite error characteristics of the spot position measurements. The new formula effectively enhances the accuracy of position measurements in a wide measurement range, which is confirmed by the simulation and experimental results. More importantly, it introduces less parameters compared with the polynomial method.

In this paper, the principle of the QD is described in Section 2. In Section 3, both the infinite integral and Boltzmann methods are briefly discussed, and the error characteristics of spot position measurements are analyzed. A new formula is proposed by combining the preceding two methods. In Section 4, a spot position measurement system and a series of experiments are described, and the verification of the new formula is given as well.

2. PRINCIPLE OF THE QD

Figure 1(a) shows the QD with an incident Gaussian beam. The QD can be regarded as being composed of four identical p–n junction photodiodes separated by small gaps. According to the photocurrent generated on each quadrant, the position of

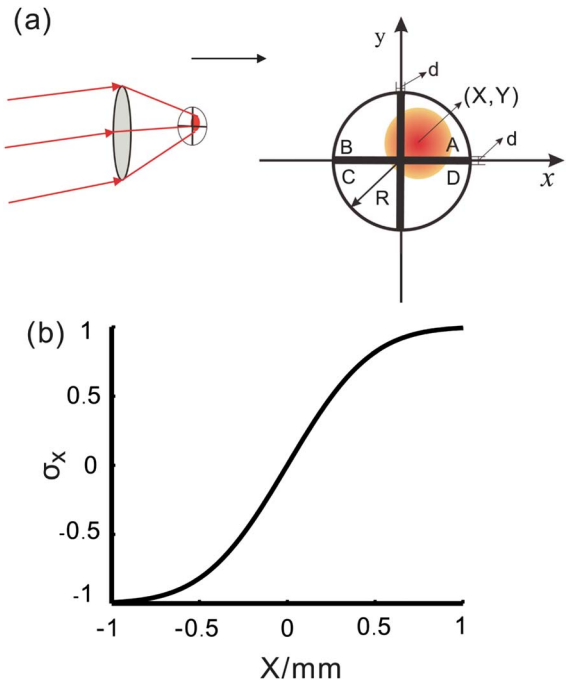

Fig. 1. (a) The QD illuminated by a Gaussian beam. (b) The relationship between σ_x and the theoretical value of spot position X.

where η is the photoelectric response ratio, Σ_i is the area of each quadrant, and $p(x, y)$ is the power intensity distribution for the Gaussian beam given by

$$p(x,y) = \frac{2P_0}{\pi\omega^2} \exp\left[-\frac{2((x-X)^2+(y-Y)^2)}{\omega^2}\right], \quad (4)$$

where P_0 is the total energy of the Gaussian beam and ω is the beam waist radius, at which point the intensity is $1/e^2$ of the maximum [17,18].

Since the response properties of the QD in the x-direction and y-direction are symmetrical, for simplification, all the following discussions focus on the x-direction, and the y-direction is similar.

The relationship between OSO σ_x in the x-direction and the spot position X can be expressed as Eq. (5) by substituting Eqs. (3) and (4) into Eq. (1), where R is the radius of QD and d is the gap between quadrants. As shown in Fig. 1(b), the OSO varies linearly with light spot position only when the spot is near the detector center and the nonlinearity increases when the spot is far from the center. In addition, the spot position X is expected to be obtained from Eq. (5), but it is difficult because it is a transcendental equation which cannot be determined analytically [19]. This is a troublesome issue to improve the measurement accuracy.

$$\sigma_x = \frac{2\left(\int_{-\sqrt{R^2-x^2}}^{\sqrt{R^2-x^2}}\int_{d/2}^{\sqrt{R^2-d^2/4}} p(x,y)\mathrm{d}x\mathrm{d}y - \int_{-d/2}^{d/2}\int_{d/2}^{\sqrt{R^2-d^2/4}} p(x,y)\mathrm{d}x\mathrm{d}y\right)}{\left(\int_{-\sqrt{R^2-x^2}}^{\sqrt{R^2-x^2}}\int_{-\sqrt{R^2-d^2/4}}^{-d/2} p(x,y)\mathrm{d}x\mathrm{d}y + \int_{-\sqrt{R^2-x^2}}^{\sqrt{R^2-x^2}}\int_{d/2}^{\sqrt{R^2-d^2/4}} p(x,y)\mathrm{d}x\mathrm{d}y - \int_{-d/2}^{d/2}\int_{-\sqrt{R^2-d^2/4}}^{-d/2} p(x,y)\mathrm{d}x\mathrm{d}y - \int_{-d/2}^{d/2}\int_{d/2}^{\sqrt{R^2-d^2/4}} p(x,y)\mathrm{d}x\mathrm{d}y\right)} - 1, \quad (5)$$

the spot center with respect to the QD center can be estimated. Arithmetically, the conventional formulas to estimate the spot position are given by

$$\sigma_x = \frac{(I_A+I_D)-(I_B+I_C)}{I_A+I_B+I_C+I_D} = \frac{2(I_A+I_D)}{I_A+I_B+I_C+I_D} - 1, \quad (1)$$

$$\sigma_y = \frac{(I_A+I_B)-(I_C+I_D)}{I_A+I_B+I_C+I_D} = \frac{2(I_A+I_B)}{I_A+I_B+I_C+I_D} - 1, \quad (2)$$

where σ_x and σ_y are defined as the OSOs in the x-direction and y-direction [11,16], respectively. I_A, I_B, I_C, and I_D are the photocurrents measured in each quadrant, respectively. The light spot center is located at (X, Y). For a single wavelength laser beam, the photocurrent on each quadrant is calculated by

$$I_i = \eta \iint_{\Sigma_i} p(x,y)\mathrm{d}x\mathrm{d}y, \quad (3)$$

3. THEORETICAL METHOD OF SPOT POSITION MEASUREMENT

A. Infinite Integral Method and Boltzmann Method

To acquire a simplified expression to calculate the real spot position value, an infinite integral method is considered. We neglect the influence of detector radius and the gap between quadrants, and then set the integral limit to infinity [20]. Thus, Eq. (5) can be simplified as

$$\sigma_x \approx \frac{2\eta\int_{-\infty}^{\infty}\int_{0}^{\infty} p(x,y)\mathrm{d}x\mathrm{d}y}{\eta\int_{-\infty}^{\infty}\int_{-\infty}^{\infty} p(x,y)\mathrm{d}x\mathrm{d}y} - 1 = \mathrm{erf}\left(\frac{\sqrt{2}X}{\omega}\right), \quad (6)$$

and then the approximate spot position x_0 can be written as

$$x_0 = \frac{\mathrm{erf}^{-1}(\sigma_x)}{\sqrt{2}} * \omega_e, \quad (7)$$

where $\mathrm{erf}^{-1}(\bullet)$ is the opposite error function. It is important to note that ω_e is defined as the effective spot radius, different from ω. ω_e can be calculated by fitting the measurement data. A further interpretation is given in Appendix A. The measurement error of the spot position δ_x is written as

$$\delta_x = x_0 - X. \tag{8}$$

The radius of a typical InGaAs QD is 1.5 mm, and the gap is around 0.045 mm. From Fig. 2(a), we can observe that x_0 obtained with the infinite integral method is always larger than X, i.e., $\delta_x > 0$ always holds in the positive direction of the x axis. Therefore, another expression with $\delta_x < 0$ is anticipated to compensate the error.

In addition, the response of the QD can also be fitted by the normalized Boltzmann sigmoidal function [21,22]. This function is denoted by

$$y = \frac{A_1 - A_2}{1 + e^{(x - x_\alpha/k)}} + A_2, \tag{9}$$

where A_1, A_2, x_α, and k are dimensionless parameters. As plotted in Fig. 3, the normalized Boltzmann sigmoidal function curve is symmetrical, where $(x_\alpha, (A_1 + A_2)/2)$ are the coordinates of the curve's center of symmetry. The parameter k determines the slope of the sigmoidal curve, and A_1 (A_2) is lower (upper) function limit. By comparing with Fig. 1(b), we are able to assign a new physical meaning to these curve parameters. As $x \to -\infty$, $\sigma_x \to -1$ and $x \to \infty$, $\sigma_x \to 1$, we can assign $A_1 = -1$, $A_2 = 1$. The symmetrical properties of the curve results in $x_\alpha = 0$. A new expression is obtained as

$$\sigma_x \approx 1 - \frac{2}{1 + e^{X/k}}, \tag{10}$$

and then the approximate spot position can be derived as

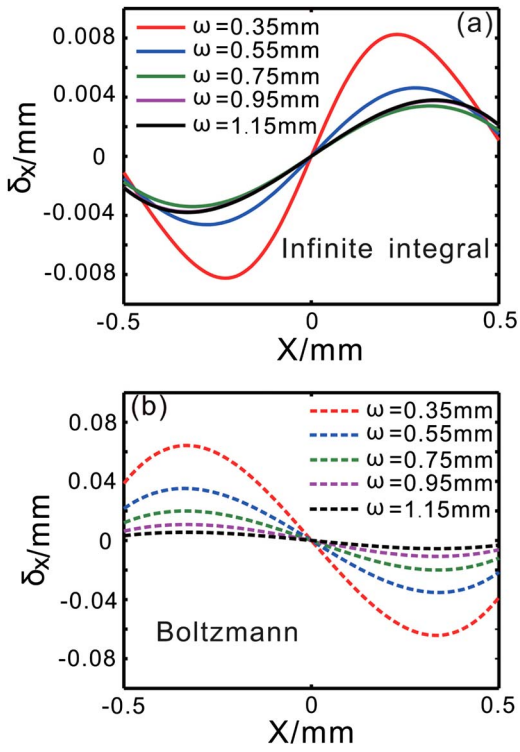

Fig. 2. Simulation results of the spot position measurement errors in (a) the infinite integral method and (b) the Boltzmann method. The measurement range of the QD is from −0.5 to 0.5 mm, and the spot radii are 0.35, 0.55, 0.75, 0.95, and 1.15 mm, respectively.

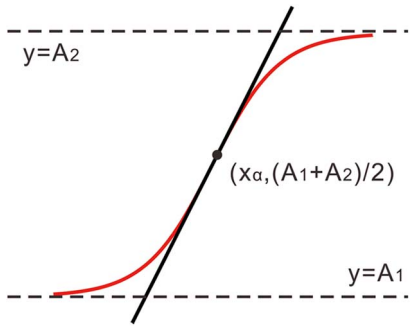

Fig. 3. Plot of the normalized Boltzmann sigmoidal function.

$$x_0 = k * \ln\left(\frac{1 + \sigma_x}{1 - \sigma_x}\right), \tag{11}$$

where the parameter k is related to the incident spot's radius, the radius of QD itself, and the gap. Eq. (11) is defined as the Boltzmann method in this paper. k can also be calculated by fitting measurement data and its further interpretation is given in Appendix A.

Fig. 2(b) shows that, in the Boltzmann method, $\delta_x < 0$ always holds in the positive direction of the x axis, i.e., the Boltzmann method has the opposite error trend with the infinite integral method. Therefore, this characteristic indicates that a linear combination of these two methods can effectively reduce the errors.

B. New Method

From Fig. 2, it can be seen that δ_x of the Boltzmann method has the opposite trend with that of the infinite integral method, as previously stated. Therefore, we establish a new formula by combining these two methods as

$$x_0(\sigma_x) = m * x_1(\sigma_x) + (1 - m) * x_2(\sigma_x), \tag{12}$$

where $x_1(\sigma_x)$ denotes the approximate spot position of the infinite integral method, and $x_2(\sigma_x)$ denotes that of the Boltzmann method. m is an adjustment parameter such that $0 < m < 1$, which can be determined using the least squares method. Therefore, N sets of data points are measured along the x-direction, and a function of the residual errors is defined as

$$\psi(m, \sigma_x) = \|\delta_x\|^2 = \sum_{i=1}^{N} [x_0(m, \sigma_{xi}) - X_i]^2, \tag{13}$$

where X_i $(i = 1, 2 \ldots N)$ is the theoretical value of the spot position, and then we let

$$\frac{\partial \psi}{\partial m} = m * \sum_{i=1}^{N} (x_1(\sigma_{xi}) - x_2(\sigma_{xi}))^2 + \sum_{i=1}^{N} (x_2(\sigma_{xi}) - X_i)(x_1(\sigma_{xi}) - x_2(\sigma_{xi})) = 0. \tag{14}$$

By solving this equation, the parameter m can be obtained as

$$m = \frac{\sum_{i=1}^{N} (X_i - x_2(\sigma_{xi}))(x_1(\sigma_{xi}) - x_2(\sigma_{xi}))}{\sum_{i=1}^{N} (x_1(\sigma_{xi}) - x_2(\sigma_{xi}))^2}. \tag{15}$$

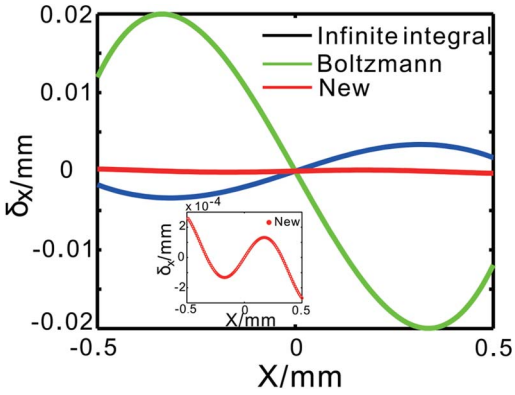

Fig. 4. Simulation results of the spot position measurement errors obtained with the infinite integral, Boltzmann, and new methods, respectively. The insert shows the close-up plot of the new method. The spot radius is 0.75 mm. The parameters of ω_e, k, and m, 0.7279, 0.2043, and 0.8545, respectively, are obtained by fitting the simulation data in the measurement range from −0.5 to 0.5 mm.

From this, we obtain the new formula in Eq. (12). Figure 4 presents the spot position measurement errors given by the three different methods when the spot radius is 0.75 mm. It can be seen that the maximum error of the new method is 0.00027 mm, which is just about one-seventieth of the Boltzmann, 0.02 mm, and about one-tenth of that of the infinite integral, 0.003 mm.

4. EXPERIMENTS AND RESULTS

A. Experiment Setup

The measurement system of the spot position using the QD is designed as Fig. 5. A laser beam (1550 nm wavelength, continuous irradiance mode semiconductor) propagates through a collimator and convex lens, and then is focused on the QD (FCI-InGaAs-Q3000, 1.5 mm detector radius and 0.045 mm gap). The beam center is located at the center of the QD by adjusting the nanopositioning stage with a position resolution of 3 nm. The total power of the laser beam is about 50 μW, which is high enough to maintain a high signal-to-noise ratio (SNR). The motion stage is controlled to move in steps of 1 μm, along the x-axis. The output voltages of each quadrant are collected by an analog–digital converter. The size of the spot radius is tuned by changing the distance between the convex lens and the QD.

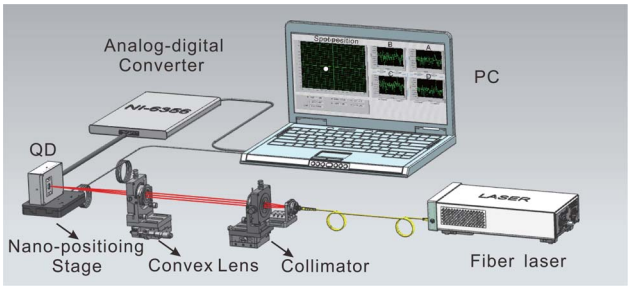

Fig. 5. Measurement system of spot position using the QD.

B. Results and Analysis

Initially, the radius of the spot is adjusted to be 0.75 mm. The spot center is shifted from −0.5 to 0.5 mm on the QD by tuning the nanopositioning stage. σ_x is calculated by Eq. (1) using the output voltage of each quadrant collected, and the theoretical spot position X is obtained by recording the values from the nanopositioning stage. Thus, from Eqs. (A7), (A8), and (15), the parameters of ω_e, k, and m are obtained as 0.733, 0.200, and 0.851, respectively.

The approximate position of the spot x_0 and the corresponding errors δ_x are then obtained using the infinite integral, Boltzmann, and new methods, respectively. Figure 6 presents the errors of the three different methods, where the experimental results agree well with the simulation. The maximum error of the new method in experiment is 0.0007 mm—as small as one-tenth of that obtained by the infinite integral method (0.007 mm) and one-thirtieth of that obtained by the Boltzmann method (0.023 mm). Furthermore, the deviation between the experimental errors and the simulation are attributed to the slight vibrations of the stage, the uneven energy distribution of the laser, and electrical noise.

In addition, to further verify the performance of the proposed new method, the errors of different spot radii are obtained with the new method. The maximum errors and the root mean square error (RMSE) of the spot position are presented in

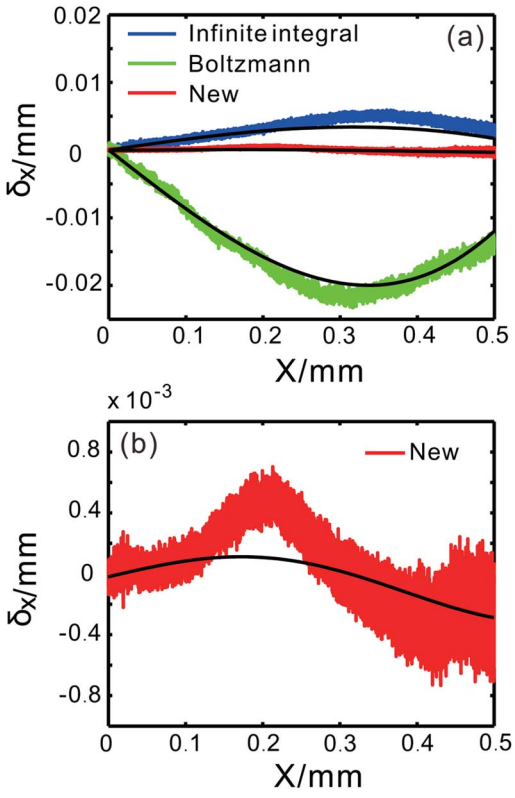

Fig. 6. (a) The simulation and experimental results of spot position measurement errors with the infinite integral, Boltzmann, and new methods, respectively. (b) Close-up plots of the new method. The measurement range is from 0 to 0.5 mm for the symmetrical characteristic of spot position errors. The black solid lines in (a) and (b) denote simulation results.

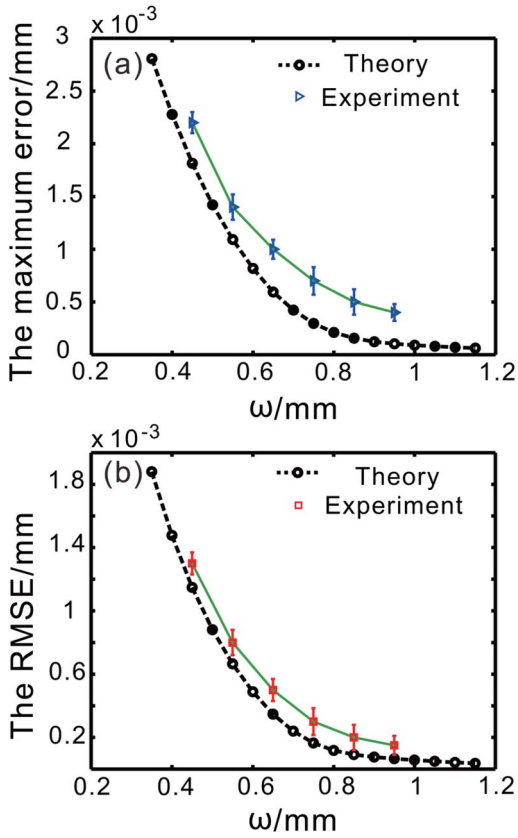

Fig. 7. (a) Maximum error and (b) the root mean square error for different spot sizes. Error bars are standard deviations for the new method from three measurements. The effective measurement range is from 0 to 0.5 mm and the spot radius varies from 0.45 to 0.95 mm.

Figs. 7(a) and 7(b), respectively. In the whole measurement area, the errors of spot position can reach as low as several micrometers. As the spot radius increases, both the maximum error and the root mean square error gradually decrease. When the spot radius is larger than 0.55 mm, the maximum error is less than 0.001 mm (relative error is less than 0.2%), and the root mean square error is less than 0.00075 mm in the measurement area.

Finally, as seen in Table 1, the number of parameters is compared between the new method and the polynomial method with nearly the same RMSE. An approximate spot position fitted by a polynomial model can be obtained as

Table 1. Number of Parameters for the New and Polynomial Methods under the Same RMSE

	Polynomial Method		Our New Method	
ω/mm	Number of Parameters	RMSE/ 10^{-4} mm	Number of Parameters	RMSE/ 10^{-4} mm
0.55	29	8.1	3	6.8
0.75	16	1.7	3	1.7
0.95	13	0.67	3	0.67
1.15	10	0.30	3	0.33

$$x_0 = A_0 + \sum_{i=1}^{n} A_i \sigma_x^i, \tag{16}$$

where n is the number of the polynomial [8,15]. For the polynomial method, the number of parameters increases when trying to achieve higher spot position precision. However, for the new method, only three parameters ω_e, k, and m are introduced. When the RMSE is the same, the new method has less parameters than the polynomial method for different spot radii.

5. CONCLUSIONS

In conclusion, a new formula has been established to determine the spot position on the QD. The simulation results show that this new formula can greatly improve the accuracy of the QD measurement with respect to different spot radii. It is also shown that our new method is robust and is well confirmed by experiment. In addition, the number of parameters is less compared with the polynomial method with the same measurement RMSE. For these advantages, the proposed method can be applied to laser communications and laser radars. Finally, this method can be also suitable for the QD with different radii and gaps.

APPENDIX A

In this section, we detail the process to achieve the effective spot radius ω_e of the infinite integral method and k of the Boltzmann method using the least squares method.

In the infinite integral method, from Eq. (6) we can obtain

$$x_0 = \frac{\mathrm{erf}^{-1}(\sigma_x)}{\sqrt{2}} * \omega. \tag{A1}$$

When taking into account the influence of the detector radius and the gap between quadrants, Eq. (A1) is improved by introducing a compensation factor $\eta\ (\omega, R, d)$:

$$x_0 = g(\sigma_x) * \omega * \eta(\omega, R, d), \tag{A2}$$

where

$$g(\sigma_x) = \frac{\mathrm{erf}^{-1}(\sigma_x)}{\sqrt{2}}, \tag{A3}$$

The effective spot radius ω_e is defined by combining ω with $\eta\ (\omega, R, d)$, and then the approximate spot position can be described as

$$x_0 = g(\sigma_x) * \omega_e. \tag{A4}$$

It is the same expression as Eq. (7). To determine ω_e, N sets of data points are measured along the x-direction; the theoretical value of the spot position is X_i, where $i = 1, 2 \ldots N$. The quadrant photocurrents are I_{Ai}, I_{Bi}, I_{Ci}, and I_{Di}, and then σ_{xi} is calculated using Eq. (1). Thus, a function describing the residual errors is set as

$$\psi(\omega_e) = \|\delta_x\|^2 = \sum_{i=1}^{N} [x_0(\omega_e) - X_i]^2, \tag{A5}$$

and then based on the least squares method, we have

$$\frac{\partial \psi}{\partial \omega_e} = 2 \sum_{i=1}^{N} g^2(\sigma_{xi}) * \omega_e - 2 \sum_{i=1}^{N} g(\sigma_{xi}) * X_i = 0. \tag{A6}$$

Finally, by solving this equation, ω_e is obtained as

$$\omega_e = \frac{\sum_{i=1}^{N} g(\sigma_{xi}) * X_i}{\sum_{i=1}^{N} g^2(\sigma_{xi})}. \quad \textbf{(A7)}$$

By a similar derivation, the parameter k in the Boltzmann method is also obtained as

$$k = \frac{\sum_{i=1}^{N} h(\sigma_{xi}) * X_i}{\sum_{i=1}^{N} h^2(\sigma_{xi})}. \quad \textbf{(A8)}$$

Funding. National Natural Science Foundation of China (NSFC) (11403064, 61102023).

Acknowledgment. The authors thank Tao Wang for the assistance rendered with the mechanical adjustment stage and appreciate useful discussions with Yue Wang in CIOMP.

REFERENCES

1. V. V. Nikulin, R. M. Khandeka, and J. SofkaAgile, "Acousto-optic tracking system for free space optical communications," Opt. Eng. **47**, 064301 (2008).
2. A. J. Mäkynen, J. T. Kostamovaara, and R. A. Myllylä, "Laser-radar based three dimensional sensor for teaching robot paths," Opt. Eng. **34**, 2596–2602 (1995).
3. L. G. Kazovsky, "Theory of tracking accuracy of laser systems," Opt. Eng. **22**, 339–347 (1983).
4. L. M. Manojlovic and Z. P. Barbaric, "Optimization of optical receiver parameters for pulsed laser-tracking systems," IEEE Trans. Instrum. Meas. **58**, 681–690 (2009).
5. S. Cui and Y. C. Soh, "Linearity indices and linearity improvement of 2-d tetralateral position-sensitive detector," IEEE Trans. Electron Devices **57**, 2310–2316 (2010).
6. J. La and K. Park, "Signal processing algorithm of a position sensitive detector using amplitude modulation/demodulation," Rev. Sci. Instrum. **76**, 024701 (2005).
7. J. Zhang, M. A. Itzler, H. Zbinden, and J.-W. Pan, "Advance in InGaAs/InP single-photon detector systems for quantum communication," Light: Sci. Appl. **4**, e286 (2015).
8. E. Silva and K. Vliet, "Robust approach to maximize the range and accuracy of force application in atomic force microscopes with nonlinear position-sensitive detectors," Nanotechnol. **17**, 5525–5530 (2006).
9. G. A. Tyler and D. L. Fried, "Image-position error associated with a quadrant detector," J. Opt. Soc. Am. **72**, 804–808 (1982).
10. M. Toyoda, K. Araki, and Y. Suzuki, "Measurement of the characteristics of a quadrant avalanche photodiode and its application to a laser tracking system," Opt. Eng. **41**, 145–149 (2002).
11. A. J. Mäkynen, J. T. Kostamovaara, and R. A. Myllylä, "Position sensitive detection techniques for manufacturing accuracy control," Proc. SPIE **1194**, 243–252 (1989).
12. L. M. Manojlović, "Quadrant photodetector sensitivity," Appl. Opt. **50**, 3461–3469 (2011).
13. T. Kubarsepp, A. Haapalinna, P. Karha, and E. Konen, "Nonlinearity measurements of silicon photodetectors," Appl. Opt. **37**, 2716–2722 (1998).
14. S. Cui and Y. C. Soh, "Improved measurement accuracy of the quadrant detector through improvement of linearity index," Appl. Phys. Lett. **96**, 081102 (2010).
15. M. Chen, Y. Yang, X. Jia, and H. Gao, "Investigation of positioning algorithm and method for increasing the linear measurement range for four-quadrant detector," Optik **124**, 6806–6809 (2013).
16. S. Cui and Y. C. Soh, "Analysis and improvement of Laguerre–Gaussian beam position estimation using quadrant detectors," Opt. Lett. **36**, 1692–1694 (2011).
17. Y. Panduputra, T. W. Ng, A. Neild, and M. Robinson, "Intensity influence on Gaussian beam laser based measurements using quadrant photodiodes," Appl. Opt. **49**, 3669–3675 (2010).
18. E. J. Lee, Y. Park, C. S. Kim, and T. Kouh, "Detection sensitivity of the optical beam deflection method characterized with the optical spot size on the detector," Curr. Appl. Phys. **10**, 834–837 (2010).
19. X. Ma, C. Rao, K. Wei, Y. Guo, and X. Rao, "Error analysis of the decrosstalk algorithm for the multianode-PMT-based quadrant tracking sensor," Opt. Express **20**, 29185–29195 (2012).
20. D. Li and S. Liu, "Research on four-quadrant detector and its precise detection," Int. J. Digital Content Technol. Appl. **5**, 138–143 (2011).
21. D. W. de Lima Monteiro, "CMOS-based integrated wavefront sensor," Ph.D. thesis, (Delft University, 2002), p. 122.
22. L. P. Salles and D. W. de Lima Monteiro, "Designing the response of an optical quad-cell as position-sensitive detector," IEEE Sens. J. **10**, 286–293 (2010).